Journal of the European Ceramic Society 20 (2000) 29–38

An analysis of microstructural parameters in the minimum contact area model for ultrasonic velocity–porosity relations

A.K. Mukhopadhyay*, K.K. Phani

Central Glass and Ceramic Research Institute, Calcutta 700 032, India

Received 31 December 1998; received in revised form 18 March 1999; accepted 26 March 1999

Abstract

The relationship between the normalised ultrasonic velocity (v/v_0) and the volume fraction (P) of pores in porous materials has been derived on the basis of a minimum solid area of contact model. It considers the development of the minimum solid area of contact during the sintering of an assembly of monosized spheres stacked in simple cubic packing. It is shown that by using a single model parameter "c", related to the effective aspect ratio "α" of spheroidal pores; it is possible to predict the trends in variation of the experimental (v/v_0 versus P) data of hot pressed silicon carbide (SiC), hot pressed silicon nitride (HPSN), reaction bonded silicon nitride (RBSN), porcelain, ceramic superconductors based on YBCO system, sintered iron and tungsten powder compacts as well as alumina. In addition, it was found that a single relation describes the behaviour of both longitudinal and transverse wave velocity as a function of pore volume fraction in all but the ceramic superconductors of the aforesaid materials. Finally, it is proposed that for all practical purposes, the analytical relation derived in the present work, can be efficiently approximated by an empirical relationship: $v/v_0 = (1 - a_1 P)^n$, where the subscript zero refers to the material of theoretical density and a_1, n are fitting parameters.

Keywords: Modelling; Ultrasonic velocity; Non-destructive evaluation; Porosity

1. Introduction

The variation of ultrasonic velocity as a function of microstructural parameters has recently emerged as a very important experimental tool to characterise the development of structural features in both green and sintered ceramics as well as sintered powder metal compacts.[1–6] The most significant microstructural parameters in this connection are the pore volume fraction (P), pore shape, their spatial orientation with respect to the stress axis and their size distribution.[3,4,6] However, theoretical attempts to model the relationship between the pore volume fraction (P) and ultrasonic velocity in sintered ceramics as well as metal powder compacts in terms of the important microstructural parameters are limited in number.[4,6]

Panakkal and co-workers[7,8] compared the observed variations in the ultrasonic velocities of sintered clay ceramic and iron powder compact with the theoretical predictions based on both linear elasticity as well as scattering theories. Large deviations were observed between the experimental data and the theoretical predictions. This was attributed to the non-spherical shape of pores. To overcome such problems Phani[9] developed a model based on the self-consistent spheroidal (SCS) inclusion theory based on effective aspect ratio (α) of the spheroids by adopting a scheme first utilised by Dean[10] to explain the modulus–porosity data of sintered ceramics; on the basis of the original theoretical work of Wu.[11] This model could explain the ultrasonic velocity versus pore volume fraction or volume fraction of second phase inclusion data on sintered iron powder compacts reported by Panakkal[8], sintered ZTA[6] and all but the data on porcelain and sintered alumina reported earlier by Roth et al.[12,13] Subsequent attempt to develop a model, which assumes the material to be a composite with cylindrical pores lying perpendicular to the stress axis[14], overestimated the data of sintered alumina[15] by as much as 10%. Very recently, Boccaccini et al.[16] have claimed better success in explaining all the data on pore volume fraction versus ultrasonic velocity used by Phani[9], by utilising a model that involves a term "z/x"

* Corresponding author. Tel.: +91-33-473-3469; fax: +91-33-473-0957.

E-mail address: anoop@cscgcri.ren.nic.in (A.K. Mukhopadhyay).

0955-2219/99/$ - see front matter
PII: S0955-2219(99)00092-8

defined as the mean axial ratio, i.e. shape factor of spheroidal pores. However, even with the application of the Mori–Tanaka theory,[17] which is based on the concept of average stress in the matrix; the predicted trend of curvature did not satisfactorily fit the experimental data on elastic moduli versus pore volume fraction ($0 < P < 0.35$) of ZnO[3].

Clearly, there is ample need to develop more precise understanding about the detailed nature of influence that the various microstructural parameters can exercise on the ultrasonic and elastic properties of sintered ceramics in general. Rice has recently expanded the consideration of actual load bearing area in this connection, on the premise that most physical properties including elastic/ultrasonic properties are determined by the minimum contact area fraction normal to the applied flux or stress.[18–20] Very recently, utilising the work of Mizusaki et al.,[21] the present authors have developed a minimum contact area (MCA) model, which gives the relationship between the normalised Young's modulus (E/E_0) and the pore volume fraction (P) developed during sintering of an idealised cubic array of monosized spheres.[22]

The purpose of the present work were: (a) to derive a relationship between the normalised ultrasonic velocity (v/v_0) and pore volume fraction (P) in terms of the adjustable parameter "c" of the MCA model,[22] (b) to examine if there is any interconnection between the parameter "c" of MCA model and the effective aspect ratio "α" of pores, considered in the SCS model,[9] (c) to show that both longitudinal and transverse ultrasonic wave velocities of brittle materials can be described by an empirical relationship $v/v_0 = (1 - a_1 P)^n$ (where a_1 and n are fitting parameters) effectively equivalent to the relationship derived from MCA concept and (d) to check the validity of the model by predicting the trend of variation in the experimental data from literature on hot pressed silicon carbide (SiC), hot pressed silicon nitride (HPSN), reaction bonded silicon nitride (RBSN), porcelain, ceramic superconductors based on YBCO system, sintered iron powder compact and sintered tungsten powder compacts of varying particle sizes.

2. Theory

The present MCA model[22] is developed on the basis of a model proposed earlier by Mizusaki et al.[21] Here, the physical picture of sintering for an idealised arrangement of monosized spheres stacked in a simple cubic array is considered. Then the model calculates the gradual change in the minimum solid area of contact between the neighbouring grains with the progress of densification, for this idealised assembly of particles. As sintering progresses, each sphere becomes welded to its six nearest neighbours. This causes shrinkage. Therefore, densification takes place along three mutually perpendicular axes. This makes the three dimensional array turn parallel to form parallelopipeds. Each of these parallelopipeds contains a uniaxial string of spheres. As the shrinkage increases, more densification occurs. This process continues until each string of spheres become a compact square bar. The assembly of these square bars generates the sintered compact. Rice[20] has recently suggested that the elastic/ultrasonic or mechanical properties of such sintered compacts are determined basically by the minimum solid area of contact. This develops at the neck between the particles along the direction of the externally applied stress. Therefore, the consideration of only one string of spheres along this stress axis becomes sufficient. Based on this premise and the related simplifying criteria[21] we have recently shown analytically that the relative density (ρ/ρ_0) is given by:[22]

$$[\rho/\rho_0] = \left[a^2 - (4ab/\pi) + \left(b^2/2\right) + (8abc/\pi)\right] \quad (1)$$

where $a = [(1 + r_0)/2]$ and $b = [(1 - r_0)/2]$. The significance of the terms "r_0" and "c" in Eq. (2) are schematically illustrated in Fig. 1. In our earlier work[22] we have already shown that for all practical purposes:

$$r_0^2 \equiv E/E_0 \quad (2)$$

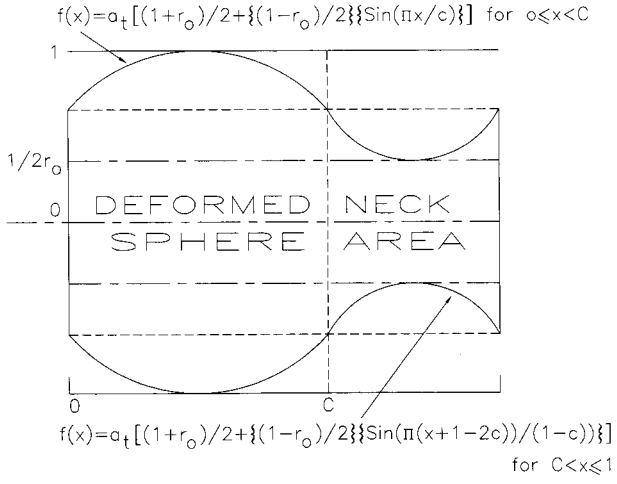

Fig. 1. This schematic presentation of the minimum contact area (MCA) model[22] is based on the work of Mizusaki et al.[21] The two sine-wave function representations are to approximate the shape of a partially deformed sphere and the developing neck area between two neighbouring spheres during sintering of monosized spheres packed in a simple cubic fashion; along with the definitions of the parameters c and r_0. Here a_t is the diameter of the deforming sphere at an instant, t.

Indeed the Eq. (2) could predict reasonably well the trend of variation in experimental data on relative Young's moduli, E/E_0 as a function of pore volume fraction in a large number of polycrystalline ceramic oxides such as Lu_2O_3, Sm_2O_3, Yb_2O_3, Al_2O_3, etc. This clearly indicates, that the relative Young's modulus is directly controlled by the normalised minimum contact area fraction, as suggested also by Rice[18–20] in the cases of a much wider variety of ceramic materials.

From physical acoustics, assuming that the ultrasonic/elastic properties are not affected to a very significant extent by the variation in Poisson's ratio with the pore volume fraction (P) in a solid of density ρ; we have the relationship between ultrasonic velocity (v) and Young's modulus given by:[6–9]

$$E = v^2\rho \tag{3}$$

and

$$E_0 = v_0^2\rho_0 \tag{4}$$

In all these equations, as mentioned earlier, the subscript "0" refers to properties of a material with theoretical density, ρ_0. Thus, we have from Eqs. (3) and (4):

$$(v/v_0) = \left[(E/E_0)/(\rho/\rho_0)\right]^{1/2} \tag{5}$$

Using Eq. (2) in Eq. (5) we get:

$$(v/v_0) = \left[(r_0)\right]/[(\rho/\rho_0)]^{1/2} \tag{6}$$

Now, the standard relationship between the pore volume fraction (P) and relative density (ρ/ρ_0) is given by:[22]

$$(\rho/\rho_0) = [1 - P] \tag{7}$$

Therefore, we have from Eqs. (1) and (7);

$$[1 - P] = \left\{a^2 - (4ab/\pi) + \left(b^2/2\right) + (8abc/\pi)\right\} \tag{8}$$

Thus, we obtain from Eqs. (6) and (7) by algebraic manipulations:

$$(v/v_0) = (r_0)/(1 - P)^{1/2} \tag{9}$$

Now, using Eq. (8) in the denominator of Eq. (9) we get:

$$(v/v_0) = (r_0)/\left[\left\{a^2 - (4ab/\pi) + \left(b^2/2\right) + (8abc/\pi)\right\}\right]^{1/2} \tag{10}$$

Therefore, substituting "a" and "b" in terms of r_0 and bearing in mind the fact that r_0 can not be a negative quantity due to physical restriction, we finally get from Eq. (10):

$$[v/v_0] = \left[\left\{1 - 64A(P - 1 + B)^{1/2}\right\} - 1\right]/\left[8A(1 - P)^{1/2}\right] \tag{11}$$

where $A = \{(3/8) - D\}$, $B = \{(3/8) + D\}$ and $D = \{(2c - 1)/\pi\}$. Clearly then, Eq. (11) predicts the variation in relative ultrasonic velocity, v/v_0, with the pore volume fraction, P using only one adjustable parameter, "c", of the minimum contact area model[22]. It has been shown in the Appendix (A3) that the analytical expression of (v/v_0) as given by Eq. (11) can be approximated effectively by the following, proposed empirical relation:

$$v/v_0 = (1 - a_1P)^n \tag{A3}$$

where both "a_1" and "n" are fitting parameters.

3. Data analysis

All data analysed earlier by Phani[9] on the basis of self-consistent spheroidal inclusion (SCS) theory and recently by Boccasini et al.[16] on the basis of "mean axial ratio" concept; were re-examined. This assemblage include data on hot pressed silicon carbide (SiC), hot pressed silicon nitride (HPSN), reaction bonded silicon nitride (RBSN), porcelain, ceramic superconductors based on YBCO system, sintered iron powder compact and sintered tungsten powder compacts of varying particle size. A computer program was run to find the best value of "c" corresponding to the best fit (solid lines in Figs. 2–11) of Eq. (11) to a given set of data. In addition, a separate computer program was run to estimate the values of the parameters "a_1" and "n" which would fit the proposed empirical Eq. (A3) to the same data the best. From these "a_1" values for different materials, the corresponding critical porosity, P_c, was found out by the expression: $P_c = (1/a_1)$. The justification for this has been given at the end of the next section.

Further, to investigate the interrelationship between the effective aspect ratio parameter "α" of the SCS model and the densification parameter "c" of the MCA model, the value of the effective aspect ratio parameter "α" was taken from Phani[9] for a given data set. All such data are given in Table 1, for the materials investigated here.

As an independent check for the validity of our proposed model and the corresponding equations, e.g. (11) and (A3), the data on ultrasonic velocity of partially sintered alumina compacts of two different initial relative density as reported earlier by Lam et al.[23] were also

re-examined. It has been shown below that our proposed model could not only predict the experimentally observed trends in variation of relative ultrasonic velocity with the pore volume fraction but also could predict the values of the critical porosities which match favourably with the experimental data.

4. Results

4.1. Silicon carbide

Fig. 2 shows the experimental data reported originally by Baaklini et al.[24] on the variation in relative longitudinal ultrasonic velocity (v/v_0) as a function of pore volume fraction (P) in hot pressed silicon carbide along with the best fitted trend ($c = 0.62$) as predicted by the present MCA model. In spite of the very small range of pore volume fraction data (0–0.12), the proposed Eq. (11) could predict the experimentally observed trend of the data. The corresponding value of effective pore aspect ratio parameter "α" was estimated out to be equal to 0.689 by Phani[9] on the basis of SCS model as mentioned earlier and is given in Table 1 along with other relevant parameters.

4.2. Silicon nitride

The experimental (v/v_0) versus P data reported originally by Maclean et al.[25] for HPSN and by Throp and

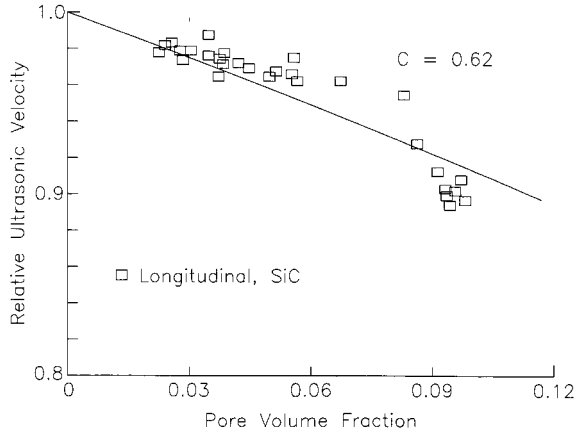

Fig. 2. Variation of relative ultrasonic velocity, v/v_0 (□, longitudinal) with pore volume fraction (P) data of hot pressed silicon carbide (HP SiC) from literature.[24] The solid line represent best fit ($c = 0.62$) to the proposed relationship [Eq. (11)] derived on the basis of the MCA model.

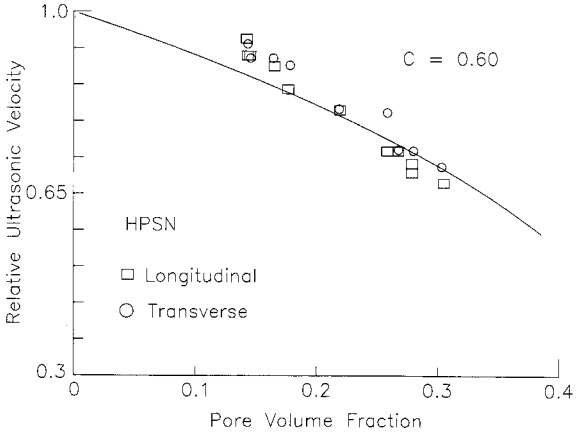

Fig. 3. Variation of relative ultrasonic velocity, v/v_0 (□, longitudinal; ○, transverse) with pore volume fraction (P) data of hot pressed silicon nitride (HPSN) from literature.[25] The solid line represent best fit ($c = 0.60$) to the proposed relationship [Eq. (11)] derived on the basis of the MCA model.

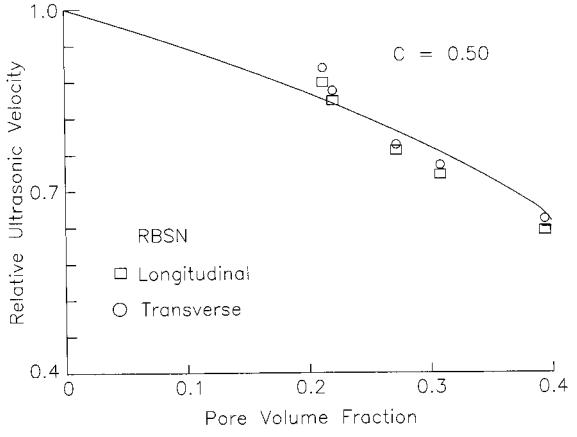

Fig. 4. Variation of relative ultrasonic velocity, v/v_0 (□, longitudinal; ○, transverse) with pore volume fraction (P) data of reaction bonded silicon nitride (RBSN) from literature.[26] The solid line represent best fit ($c = 0.50$) to the proposed relationship [Eq. (11)] derived on the basis of the MCA model.

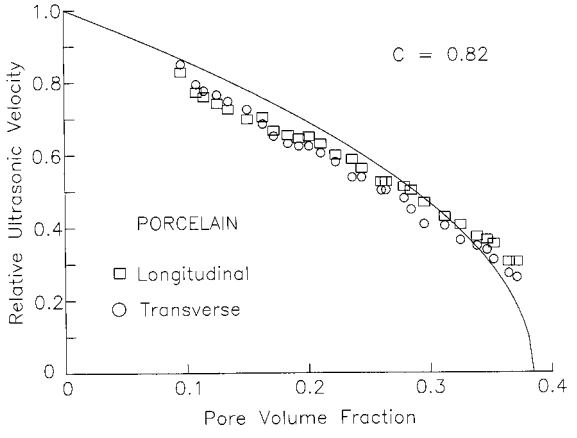

Fig. 5. Variation of relative ultrasonic velocity, v/v_0 (□, longitudinal, ○, transverse) with pore volume fraction (P) data of porcelain from literature.[27] The solid line represent best fit ($c = 0.82$) to the proposed relationship [Eq. (11)] derived on the basis of the MCA model.

Bushell[26] for RBSN along with the best fitted trend ($c = 0.6$, $c = 0.5$) are shown in Figs. 3 and 4, respectively. In both of these cases, the predicted trends match with the experimental data. Further, in each of these cases, one singular "c" value could predict the experimentally observed trends of variation in both longitudinal and transverse velocities as a function of the corresponding pore volume fraction data; as predicted according to the current MCA model, Eq. (11). The "α" values as estimated from SCS model[9] are 0.441 and 0.621 for HPSN and RBSN, respectively.

4.3. Porcelain

The trends of variation in experimental (v/v_0) versus P data on Porcelain[27] along with the best fitted trend [$c = 0.82$, Eq. (11)] are shown in Fig. 5. For both longitudinal and transverse velocities the predicted trends match with the experimental data. Here, "α" is 0.150[9].

4.4. Ceramic superconductor ($YBa_2Cu_3O_{7-x}$)

The trends of variation in the experimental (v/v_0) versus P data[28–32] of $YBa_2Cu_3O_{7-x}$ samples; along with the best fitted trend [$c = 0.60$, $c = 0.73$; Eq. (11)] are shown in Fig. 6. The predicted trends match with the experimental data. However, two different "c" values (0.60 and 0.73) were needed to achieve this. The reason may be that (i) the experimental data was not from a singular source, (ii) the different YBCO samples were also synthesised using a wide variety of starting powder

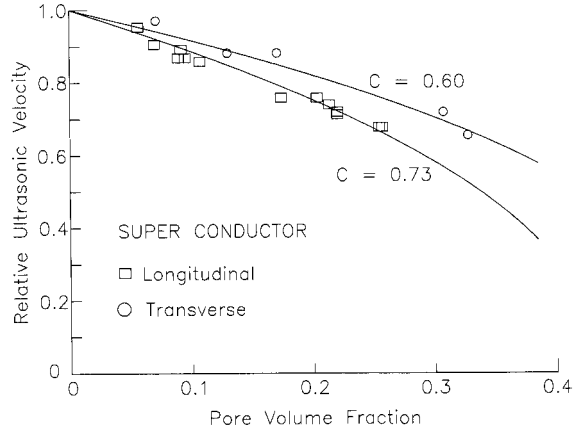

Fig. 6. Variation of relative ultrasonic velocity, v/v_0 (□, longitudinal; ○, transverse) with pore volume fraction (P) data of $YBa_2Cu_3O_{(7-x)}$ from literature.[28–32] The solid line represent best fit ($c = 0.73$ for longitudinal, $c = 0.60$ for transverse velocity data) to the proposed relationship [Eq. (11)] derived on the basis of the MCA model.

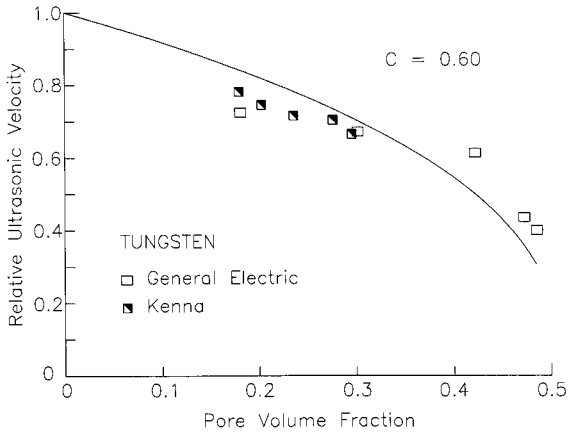

Fig. 8. Variation of relative ultrasonic velocity, v/v_0 (longitudinal: □, General Electric powder; ■, Kenna powder) with pore volume fraction (P) data of sintered tungsten powder compacts (initial particle size 4 μm) from literature.[33] The solid line represent best fit ($c = 0.60$) to the proposed relationship [Eq. (11)] derived on the basis of the MCA model.

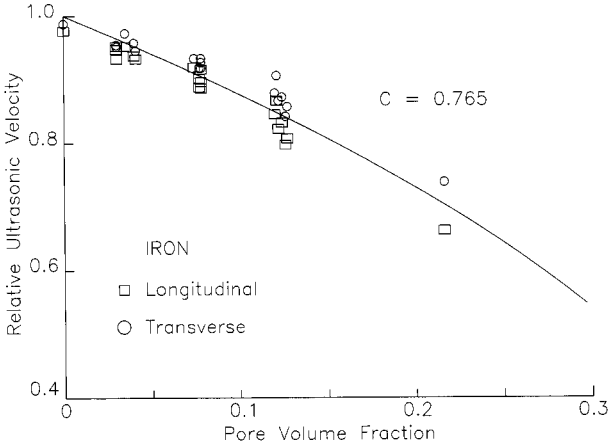

Fig. 7. Variation of relative ultrasonic velocity, v/v_0 (□, longitudinal; ○, transverse) with pore volume fraction (P) data of sintered iron powder compacts from literature.[8] The solid line represent best fit ($c = 0.765$) to the proposed relationship [Eq. (11)] derived on the basis of the MCA model.

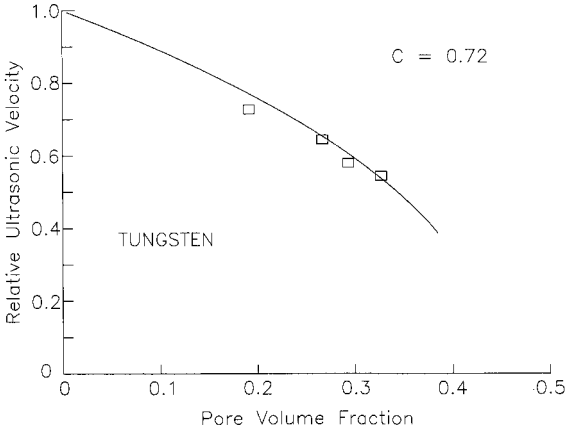

Fig. 9. Variation of relative ultrasonic velocity, v/v_0 (□, longitudinal) with pore volume fraction (P) data of sintered tungsten powder compacts (initial particle size 18 μm) from literature.[33] The solid line represent best fit ($c = 0.72$) to the proposed relationship [Eq. (11)] derived on the basis of the MCA model.

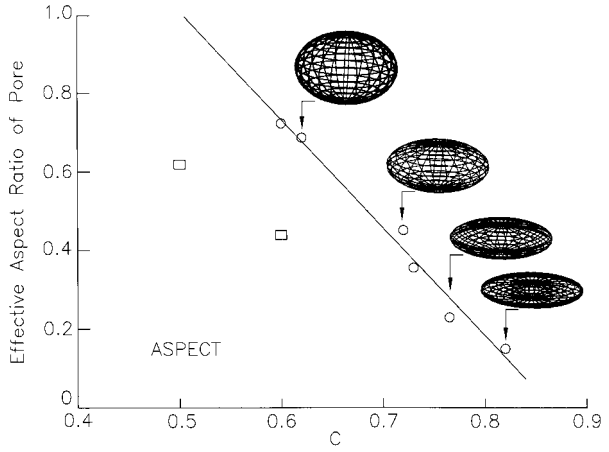

Fig. 10. Linear relationship between the effective pore aspect ratio (α) of spheroidal pores as estimated by the SCS Model[9] and the "Densification Parameter (c)" from the MCA model. The solid line represents Eq. (15). Insets show the change in the pore shape as the value of α increases from a value close to zero (pore shape more oblate spheroidal) to a value close to unity (pore shape more spheroidal); consequent to the changes in the value of the Densification Parameter (c).

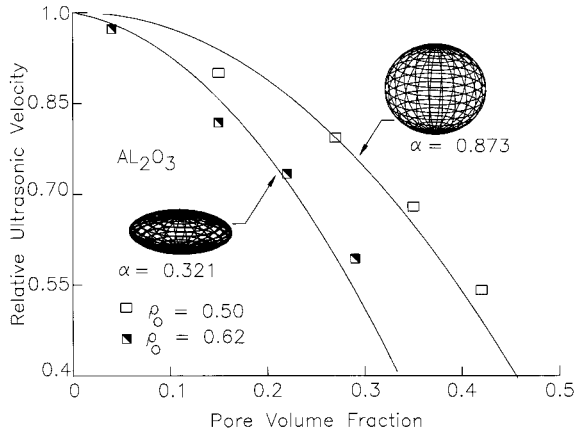

Fig. 11. Variation of relative longitudinal ultrasonic velocity, v/v_0 with pore volume fraction (P) data of partially sintered alumina powder compacts having two different relative initial green density (ρ_0) values (□, $\rho_0 = 0.50$; ◪, $\rho_0 = 0.62$) from literature.[23] The solid lines represent best fit ($\alpha = 0.321$ for $\rho_0 = 0.62$ and $\alpha = 0.873$ for $\rho_0 = 0.50$) according to the SCS Model[9] The α values were determined on the basis of the MCA model, Eq. 15).

particle sizes, purity and fabrication techniques; thereby introducing sources of random fluctuations in the raw data itself. From SCS model of Phani[9] the "α" value is estimated to be 0.357.

4.5. Sintered iron powder compact

The trends of variation in the experimental (v/v_0) versus P data of sintered iron powder compact[9] along with the best fitted trend [$c = 0.765$, Eq. (11)] are shown in Fig. 7. For both longitudinal and transverse velocities, the predicted trends match with the experimental data. The "α" value as estimated from SCS model[9] is 0.273.

Table 1
Model parameters for different materials

Material	c	a_1	n	P_{cr}	α
SiC	0.620	2.0058	0.4070	0.4985	0.689
HPSN	0.600	1.9580	0.3971	0.5107	0.441
RBSN	0.500	1.7499	0.3483	0.5700	0.621
Porcelain	0.820	2.5986	0.5048	0.3850	0.150
Superconductor (v_l)	0.730	2.3062	0.4608	0.4336	0.357
Superconductor (v_s)	0.600	1.9200	0.4100	0.5200	0.357
Iron	0.765	2.4149	0.4779	0.4141	0.273
Tungsten (4 μm)	0.600	1.9200	0.4100	0.5200	0.725
Tungsten (18 μm)	0.720	2.2763	0.4559	0.4393	0.453
Alumina ($\rho_0 = 0.50$)	0.550	1.8475	0.3728	0.5443	0.873
Alumina ($\rho_0 = 0.62$)	0.750	2.3675	0.4701	0.4223	0.321

4.6. Sintered tungsten powder compact

The trends of variation in experimental (v/v_0) versus P data of sintered tungsten powder compact[33] along with the best fitted trends [$c = 0.60$, 4 μm particle size and $c = 0.72$, 18 μm particle size; Eq. (11) are shown in Figs. 8 and 9. The "α" values as estimated from SCS model of Phani[9] are 0.725 and 0.453 for data presented in Figs. 8 and 9, respectively.

5. Discussion

Based on the data of Table 1, the following best fitted empirical equations could be obtained:

$$a = 1.49 - 0.77c + 2.60c^2 \tag{12}$$

$$n = 0.49c + 0.10 \tag{13}$$

$$P_c = 0.85 - 0.58c \tag{14}$$

and

$$\alpha = 2.39 - 2.75c \tag{15}$$

The last of these equations [Eq. (15)] is obviously the most important because it gives a linear relationship between the "effective pore aspect ratio α" of the SCS model[9] and the "densification parameter c" of the MCA model.[22] This unique relationship is depicted as a solid line in Fig. 10. It may be noted that the data of both the silicon nitride ceramics (HPSN and RBSN) were away from the general trend. The exact reason for this is yet to be known. However, it may be guessed that in the case of RBSN, the pore shape would be dependent on

those present in the initial, green Si powder compact and the kinetics of nitridation. Similarly, in the case of HPSN, the actual pore shapes may be quite complex due to the usual presence of sintering aids which affects densification and hence, pore shrinkage. Hence, the corresponding "c" data were excluded while obtaining Eq. (15). The change in pore shape as reflected by the change in the values of "α" are shown as insets in Fig. 10.

Altogether 9 different sets of data have been analysed in the present work. All these data could be predicted reasonably close to what have been experimentally observed; by using Eq. (11). In all these cases the data on both relative longitudinal and relative transverse ultrasonic velocities could be explained by the singular "c" values (Figs. 2–5, 7–9) in complete conformity with the model developed here; except for the data on YBCO ceramic superconductor; the reasons for which has been discussed earlier (Sub-section 4.4). These observations lend credence to the validity of the proposed MCA model and the corresponding equations.

In addition, it may be noted from Fig. 10 that the lower the "c" value the higher is the effective aspect ratio of the pore meaning that at lower values of "c" the microstructure consists of more spheroidal pores which, in turn, enhances densification. This gives the physical significance of the parameter "c" in the proposed MCA model. It may be seen from Eq. (15) that at $c = 0.87$, the value of "α" becomes zero, i.e. oblate spheroids would reduce to disc shape at such stage and prolate spheroids would correspondingly become more needle shaped, as is also evident from Fig. 10. Similarly, at a value of $c \approx 0.51$, the value of α becomes unity, i.e. then the spheroidal pore assumes exactly the shape of a sphere.

To check further the validity of the present MCA model independently, the data of Lam et al.[23] on the variation of relative ultrasonic velocity of partially sintered alumina compacts have been used in Fig. 11. Here, the "effective pore aspect ratio" data was initially obtained for the two sets of alumina compacts with two different initial relative density values ($\rho_0 = 0.50$ and 0.62) using the calibration Eq. (15) with the best fitted "c" values according to Eq. (11) of the present MCA model. Then, these newly found values of "α" were used in the SCS scheme developed by Phani[9] to predict the variation in the experimental data[23] on relative longitudinal ultrasonic wave velocity as a function of the pore volume fraction. The results are shown in Fig. 11.

The predicted trends (Fig. 11) show agreement with the experimental data. That implies that the corresponding "c" values which were used to predict these "α" values are reasonable and hence, the validity of Eq. (11). Further, the predicted values of critical porosity are in reasonable match with the experimental data (cf. theoretically predicted P_{cr} is 0.54; experimental P_{cr} is 0.50; theoretically predicted P_{cr} is 0.42; experimental P_{cr} is 0.38, Table 1).

The insets of Fig. 11 show the two very different pore geometries involved in these two alumina compacts[23]. Notice that the compact with lower value of initial relative density (hollow rectangle, Fig. 11) had a very high value of effective pore aspect ratio, i.e. $\alpha = 0.873$, implying that the spheroidal pores were almost close to sphere ($\alpha = 1$) in shape. Such a starting microstructure, would obviously have, at least initially, a faster densification rate, and hence; higher values of relative longitudinal ultrasonic velocity in comparison to one with the prolate spheroidal pore shape ($\alpha = 0.321$, Fig. 11). This second type of microstructure will have, at least initially, a lower rate of densification in spite of having a higher relative green density ($\rho_0 = 0.62$[23]) and hence; a comparatively lower value of relative longitudinal ultrasonic velocity at comparable levels of pore volume fractions except at very low P values. Thus, our predicted trends are in reasonable agreement with the experimentally observed data (Fig. 11). Such agreement assumes considerable significance in view of the fact that a single effective aspect ratio "α" of the pores could describe the correlation of ultrasonic velocity with porosity data over a wide range eg. as in the case of the data on porous alumina[23] considered here. Hence, this point is worth some clarification.

It should be borne in mind that if the microstructures of a batch of real, sintered material are considered; more often than not the individual members will have a large, wide range of porosities. Indeed, in such cases, the real, individual pores can have aspect ratios varying anywhere in the range 0 to 1. Following the work of Dean[10] and Phani,[9] however, the effect of such real pores on the ultrasonic velocity can be reasonably approximated by consideration of a "equivalent, conceptual" sintered material containing the same volume fraction (P) of pores such that all the individual pores have one and the same aspect ratio, defined as the "effective aspect ratio", α. The present work is based on this premise of the SCS model.[9,10] Therefore, for a given set of data for a given material, the parameter called "effective aspect ratio", α remains a constant. In accordance with Eq. (15) obtained in the present work this constancy of α implies in turn, the constancy of the densification parameter "c", which, for a given set of data for a given material is essentially determined by the initial particle size of the powder being sintered and their packing geometry in the green compact. This fact is evident from the data given in Table 1 for the cases of sintered tungsten powder compact[33] and partially sintered alumina.[23] The case of partially sintered alumina has been already discussed. For tungsten powder of 4 μm initial particle size, the effective aspect ratio of pores is 0.725 and hence, c is 0.6. However, for the same tungsten material with a larger initial particle size e.g. 18

μm the effective aspect ratio becomes 0.453 and hence c is 0.720. Thus, in the former situation, the equivalent sintered material contains more of spheroidal pores whereas in the later situation it contains more of prolate spheroidal pores. As densification proceeds, it is the parameter r_0 which changes, thus changing the shape of the pores.

Finally, it may be recalled that the values of P_{cr} are calculated as $P_{cr} = (1/a_1)$. It follows from Eq. (A3) that at a critical porosity $P = P_{cr} = (1/a_1)$, the quantity on the right hand side of (A3) vanishes i.e. (v/v_0) becomes equal to zero. This is the critical porosity level, beyond which, the ultrasonic velocity becomes zero in the material implying that at $P > P_{cr}$, the attenuation is so high that effectively no velocity can be measured. In this connection, it may be mentioned that Phani and co-workers [34,35] have empirically proposed earlier a similar relationship, viz.:

$$v/v_0 = (1 - P)^m \tag{16}$$

to explain the data on gypsum as well as sintered metal powder compacts. In the Eq. (16), the quantity "m" is an empirical parameter to be obtained by data fitting technique.

Now, it is apparent from our Eq. (A3) that it is the generalised form of Eq. (16), proposed by earlier workers.[34,35] Further, the parameters "a_1" and "n" are found out here to be linked to "c" (cf. Eqs. 12 and 13, respectively). The parameter "c" bears the physical significance of a "densification parameter" as mentioned earlier.

Before the final conclusions can be drawn, an important aspect of the present work needs to be emphasized. Unless "c" can be experimentally determined, the prediction potential of the present model [Eq. (11)] can not be fully realised. But, the experimental determination of "c" in the case of real porous structures is not an easy task at the moment. This, in turn, may impose some limitation on more widespread applications of the present model for actual prediction, rather than only fitting of the ultrasonic velocity and hence, elastic constant data of porous solids. It is interesting to note however, that in spite of such limitations the densification parameter "c" of the present MCA model could still predict the values of real, physical bounds of the effective pore aspect ratio "α" i.e. at $c = 0.87$, "α" = 0 and at $c \approx 0.51$, "α" = 1.

6. Conclusions

The major conclusions of the present work are as follows:

a. The relationship between the normalised ultrasonic velocity (v/v_0) and the volume fraction (P) of pores in porous materials has been derived on the basis of a minimum solid area of contact (MCA) model. The model considers the development of the minimum solid area of contact during the sintering of an assembly of monosized spheres stacked in simple cubic packing.
b. Using the present MCA model it was possible to predict the trends of variation in experimental data on relative longitudinal as well as transverse ultrasonic wave velocities as a function of pore volume fraction in SiC, HPSN, RBSN, porcelain, $YBa_2Cu_3O_{7-x}$ ceramic superconductors, and sintered iron as well as tungsten powder compacts of varying particle sizes.
c. The trends of variation in the experimental (v/v_0) versus P data of partially sintered alumina compacts reported in the literature could be predicted in an independent fashion, utilising the relationship between the densification parameter "c" of the current MCA model and "α", the effective pore aspect ratio of SCS model.
d. The relationship between (v/v_0) and P [Eq. (11)] describes the behaviour of both longitudinal and transverse wave velocity in all but the ceramic superconductors of the materials investigated here.
e. For all practical purposes, the relationship:

$$[v/v_0] = \left[\left\{1 - 64A(P - 1 + B)^{1/2}\right\} - 1\right]/\left[8A(1 - P)^{1/2}\right]$$

derived in the present work (A and B are both functions of the densification parameter c), can be effectively approximated by the proposed empirical relationship:

$$[v/v_0] = (1 - a_1 P)^n$$

where the subscript zero refers to the material of theoretical density and a_1, n are fitting parameters.

Appendix

From Eq. (8), replacing "a" and "b" in terms of r_0, and remembering that $\rho/\rho_0 = (1 - P)$; we obtain the following quadratic in terms of r_0:

$$Ar_0^2 + (1/4)r_0 + \left\{B - (1 - P)\right\} = 0 \tag{A1}$$

where $A = [(3/8) - D]$, $B = [(3/8) + D]$, and $D = (2c - 1)/\pi$. Now, solving Eq. (A1) for r_0 in view of the physical boundary condition that r_0 can not be negative as the densification occurs during the course of sintering and utilising the same in Eqs. (9) and (11); we obtain after simplification:

$$[v/v_0] = 1 + \{(3-2D)/2(1-2D)\}P + [\{4(1-2D)^2 - (3-8D) + 3(1-2D)^3\}/\{8(1-2D)\}^3]P^2 + \text{higher order terms} \quad \text{(A2)}$$

The right hand side of Eq. (A2) can be approximated effectively by the empirical relationship:

$$[v/v_0] = (1 - a_1 P)^n \quad \text{(A3)}$$

References

1. Schilling, C. H., Garcia, V. J., Smith, R. M. and Roberts, R. A., Ultrasonic and mechanical behaviour of green and partially sintered alumina: effects of slurry consolidation chemistry. *J. Am. Ceram. Soc.*, 1998, **81**, 2629–2639.
2. Kathrina, T. and Rawlings, R. D., Non destructive evaluation of porous MgO ceramics using acoustic techniques. *J. Mater. Sci.*, 1997, **32**, 3951–3960.
3. Martin, L. P. and Rosen, M., Correlation between surface area reduction and ultrasonic velocity in sintered zinc oxide powders. *J. Am. Ceram. Soc.*, 1997, **80**, 839–846.
4. Martin, L. P., Doden, D. and Rosen, M., Evaluation of ultrasonically determined elasticity porosity relation in zinc oxide. *J. Am. Ceram. Soc.*, 1996, **79**, 1281–1289.
5. Kathrina, T. and Rawlings, R. D., Acoustic studies of the effect of SiC particle reinforcement on the compaction of alumina powder. *J. Eur. Ceram. Soc.*, 1997, **17**, 1157–1167.
6. Phani, K. K., Mukherjee, S. and Basu, D., Ultrasonic characterisation of zirconia toughened alumina ceramics. *J. Am. Ceram. Soc.*, 1996, **79**, 3331–3335.
7. Panakkal, J. P., Nondestructive characterisation of clay ceramics using ultrasonics. *Br. J. NDT*, 1992, **34**, 529–532.
8. Panakkal, J. P., Willems, H. and Arnold, W., Non-destructive evaluation of elastic parameters of sintered iron powder compacts. *J. Mater. Sci.*, 1990, **25**, 1397–1402.
9. Phani, K. K., Porosity-dependence of ultrasonic velocity in sintered materials—a model based on the self-consistent spheroidal inclusion theory. *J. Mater. Sci.*, 1996, **31**, 272–279.
10. Dean, E. A., Elastic moduli of porous sintered materials as modeled by a variable-aspect-ratio self-consistent oblate-spheroidal-inclusion theory. *J. Am. Ceram. Soc.*, 1983, **66**, 847–854.
11. Wu, T. T., The effect of inclusion shape on elastic moduli of a two-phase material. *Int. J. Solids Struct.*, 1966, **2**, 1–8.
12. Roth, D. J., Stang, D. B., Swickard, S. M. and DeGuire, M. R., Review and statistical analysis of the ultrasonic velocity method for estimating the porosity fraction in polycrystalline materials, NASA technical memorandum no. 102501, 1990.
13. Roth, D. J., Stang, D. B., Swickard, S. M., DeGuire, M. R. and Dolhert, L. E., Review, modeling and statistical analysis of ultrasonic velocity-pore fraction relations in polycrystalline materials. *Mater. Eval.*, 1991, **49**, 883–888.
14. Phani, K. K., Porosity dependence of elastic properties and ultrasonic velocity in polycrystalline alumina—a model based on cylindrical pores. *J. Mater. Sci.*, 1996, **31**, 262–266.
15. Nagarajan, A., Ultrasonic study of elasticity-porosity relationship in polycrystalline alumina. *J. Appl. Phys.*, 1971, **42**, 3693–3696.
16. Boccaccini, D. N. and Boccaccini, A. R., Dependence of ultrasonic velocity on porosity and pore shape in sintered materials. *J. Non Destructive Evaluation*, 1997, **16**, 187–192.
17. Mori, T. and Tanaka, K., Average stress in matrix and average elastic energy of materials with misfitting inclusions. *Acta Metall.*, 1973, **21**, 571–574.
18. Rice, R. W., Evaluating porosity parameters for porosity-property relations. *J. Am. Ceram. Soc.*, 1993, **76**, 1801–1805.
19. Rice, R. W., Evaluation and extension of physical property-porosity based on minimum solid area. *J. Mater. Sci.*, 1996, **31**, 102–118.
20. Rice, R. W., Comparison of stress concentration versus minimum solid area based on mechanical property-porosity relations. *J. Mater. Sci.*, 1993, **28**, 2187–2190.
21. Mizusaki, J., Tsuchiya, S., Waragai, K., Tagawa, H., Arai, Y. and Kuwayama, Y., Simple mathematical model for the electrical conductivity of highly porous ceramics. *J. Am. Ceram. Soc.*, 1996, **79**, 109–113.
22. Mukhopadhyay, A. K. and Phani, K. K., Young's modulus - porosity relations: an analysis based on a minimum contact area model. *J. Mater. Sci.*, 1998, **33**, 69–72.
23. Lam, D. C. C., Lange, F. F. and Evans, A. G., Mechanical properties of partially dense alumina produced from powder compacts. *J. Am. Ceram. Soc.*, 1994, **77**, 2113–2117.
24. Baaklini, G. Y., Generazo, E. R. and Kiser, J. D., High frequency ultrasonic characterisation of sintered silicon carbide, *J. Am. Ceram. Soc.*, 1989, **72**, 383–387.
25. Mclean, A. F. et al., Brittle materials design, high temperature gas turbine. Interim report number 7, 1 July, 1974 to 31 December, 1974. AMMRC CTR 75–8, 1975, p. 97.
26. Thorp, J. S. and Bushell, T. G., Ultrasonic examination of reaction bonded silicon nitride. *J. Mater. Sci.*, 1985, **20**, 2265–2274.
27. Boisson, J., Platon, F. and Boch, P., Constanti electriche E. Attrito interno in alconi materials in funzione della porosita. *Ceramurgia*, 1976, **6**, 74–76.
28. Blendell, J. E., Chiang, C. K., Cranmer, D. C., Freiman, S. W., Fuller, E. R. Jr., Krasicka, E. D., Johnson, W. L., Ledbetter, H. M., Benett, L. H., Swatzchdriber, L. J., Marinenko, R. B., Myklebust, R. L., Bright, D. S. and Newbury, D. E., Processing–property relations for $Yba_2Cu_3O_{(7-x)}$ high T_c superconductors. *Adv. Ceram. Mater.*, 1987, **2**, 512–529.
29. Gaiduk, A. L., Zherlitsyn, S. V., Prikhodko, O. R., Seminozhenko, V. P., Nesterenko, V. F. and Pershin, S. A., High frequency acoustic properties of yttrium ceramic. *Sov. J. Low Temp. Physics*, 1988, **14**, 395–402.
30. Roth, D. J., Dolhert, L. E. and Kerwin, D. P., Unpublished research. NASA Lewis Research Center, Cleveland, OH, 1990.
31. Round, R. and Bridge, B., Elastic constants of the high temperature ceramic superconductor $YBa_2Cu_3O_{(7-x)}$. *J. Mater. Sci. Lett.*, 1987, **6**, 1471–1472.

32. Ledbetter, H. M., Austin, M. W., Kim, S. A. and Lei, M., *J. Mater. Res.*, 1987, **2**, 786.
33. Smith, J. T. and Lopilato, S. A., The correlation of density of porous tungsten billets and ultrasonic wave velocity. *Trans. Metall. Soc., AMIE*, 1966, **236**, 597–598.
34. Maitra, A. K. and Phani, K. K., Ultrasonic evaluation of elastic parameters of sintered iron powder compacts. *J. Mater. Sci.*, 1994, **29**, 4415–4419.
35. Phani, K. K., Young's modulus-porosity relation in gypsum systems. *Am. Ceram. Soc. Bull.*, 1986, **65**, 1584–1586.